Fungal Small RNAs Suppress Plant Immunity by Hijacking Host RNA Interference Pathways

Arne Weiberg *et al.*

Science **342**, 118 (2013);
DOI: 10.1126/science.1239705

Science (print ISSN 0036-8075; online ISSN 1095-9203) is published weekly, except the last week in December, by the American Association for the Advancement of Science, 1200 New York Avenue NW, Washington, DC 20005.

16. S. Isayenkov, F. J. Maathuis, *Plant Signal. Behav.* **8**, e24665 (2013).
17. M. Zanetti *et al.*, *PLOS ONE* **5**, e10118 (2010).
18. S. de Bianchi *et al.*, *Plant Cell* **23**, 2659–2679 (2011).
19. B. Bailleul, P. Cardol, C. Breyton, G. Finazzi, *Photosynth. Res.* **106**, 179–189 (2010).
20. J. A. Cruz, C. A. Sacksteder, A. Kanazawa, D. M. Kramer, *Biochemistry* **40**, 1226–1237 (2001).
21. S. Eberhard, G. Finazzi, F. A. Wollman, *Annu. Rev. Genet.* **42**, 463–515 (2008).
22. N. E. Ioannidis, J. A. Cruz, K. Kotzabasis, D. M. Kramer, *PLOS ONE* **7**, e29864 (2012).
23. T. J. Avenson, J. A. Cruz, D. M. Kramer, *Proc. Natl. Acad. Sci. U.S.A.* **101**, 5530–5535 (2004).
24. N. V. Paramonova, N. I. Shevyakova, V. V. Kuznetsov, *Russ. J. Plant Physiol.* **51**, 86–96 (2004).
25. E. Rintamäki, P. Martinsuo, S. Pursiheimo, E. M. Aro, *Proc. Natl. Acad. Sci. U.S.A.* **97**, 11644–11649 (2000).
26. G. Schönknecht, R. Hedrich, W. Junge, K. Raschke, *Nature* **336**, 589–592 (1988).
27. M. Tester, M. R. Blatt, *Plant Physiol.* **91**, 249–252 (1989).
28. K. Maxwell, G. N. Johnson, *J. Exp. Bot.* **51**, 659–668 (2000).

Acknowledgments: The authors are grateful to M. Zoratti and N. La Rascio for useful discussion and to J. Barber, N. Uozumi, P. Joliot, and N. Rolland for critical reading of the manuscript. We thank A. Spena for the pBIN RolC plasmid, L. Leanza for help with antibody production, and M. Simonetti for help with artwork. We thank Italy's PRIN (Research Projects of National Interest) (2010CSJX4F_005 to I.S.) and European Molecular Biology Organization Young Investigator Program for financial support (to I.S.) and the Aldo Gini Program for a short-term grant to V.C. to work in the laboratory of G.F.; the Ph.D. fellowship for L.C. was provided by the Italian Ministry of Education (L170). M.T. was supported by the French National Agency (ANR-2010-GENOM-BTV-002-01 Chloro-Type). G.F. was funded by the French National Agency "Project PhytAdapt" (ANR-NT09_567009), the Marie Curie Initial Training Network "AccliPhot" (FP7-PEPOPLE-2012-ITN, grant agreement number 316427), and the Labex GRAL (Grenoble Alliance for Integrated Structural Cell Biology) grants. Author contributions: expression and purification of AtTPK3: L.C. and E.T.; electrophysiology: L.C., E.T., and I.S.; localization: L.C., E.F., and M.T.; silencing: L.C. and E.F.; pigment analysis: L.C. and T.M.; analysis of visible phenotype: L.C., T.M., I.S., and G.F.; electron microscopy and transmission electron microscopy service: L.C.; pmf measurements: M.T., V.C., and G.F. The study was designed by I.S., G.F., and G.M.G.; the paper was written by I.S. and G.F. This paper is dedicated to G. Franchin and E. Vaccher at Centro di Riferimento Oncologico (CRO), Aviano. Authors declare no conflict of interest. Additional data are in the supplementary materials.

Supplementary Materials

www.sciencemag.org/content/342/6154/114/suppl/DC1
Materials and Methods
Figs. S1 to S9
Tables S1 and S2
References (*29*–*42*)

18 June 2013; accepted 27 August 2013
Published online 5 September 2013;
10.1126/science.1242113

Fungal Small RNAs Suppress Plant Immunity by Hijacking Host RNA Interference Pathways

Arne Weiberg,[1,2,3]* Ming Wang,[1,2,3]* Feng-Mao Lin,[4] Hongwei Zhao,[1,2,3]† Zhihong Zhang,[1,2,3,5] Isgouhi Kaloshian,[2,3,6] Hsien-Da Huang,[4,7] Hailing Jin[1,2,3]‡

***Botrytis cinerea*, the causative agent of gray mold disease, is an aggressive fungal pathogen that infects more than 200 plant species. Here, we show that some *B. cinerea* small RNAs (Bc-sRNAs) can silence *Arabidopsis* and tomato genes involved in immunity. These Bc-sRNAs hijack the host RNA interference (RNAi) machinery by binding to *Arabidopsis* Argonaute 1 (AGO1) and selectively silencing host immunity genes. The *Arabidopsis ago1* mutant exhibits reduced susceptibility to *B. cinerea*, and the *B. cinerea dcl1 dcl2* double mutant that can no longer produce these Bc-sRNAs displays reduced pathogenicity on *Arabidopsis* and tomato. Thus, this fungal pathogen transfers "virulent" sRNA effectors into host plant cells to suppress host immunity and achieve infection, which demonstrates a naturally occurring cross-kingdom RNAi as an advanced virulence mechanism.**

Botrytis cinerea is a fungal pathogen that infects almost all vegetable and fruit crops and annually causes $10 billion to $100 billion in losses worldwide. With its broad host range, *B. cinerea* is a useful model for studying the pathogenicity of aggressive fungal pathogens. Many pathogens of plants and animals deliver effectors into host cells to suppress host immunity (*1*–*4*). All the pathogen effectors studied so far are proteins. We found that small RNA (sRNA) molecules derived from *B. cinerea* can act as effectors to suppress host immunity.

sRNAs induce gene silencing by binding to Argonaute (AGO) proteins and directing the RNA-induced silencing complex (RISC) to genes with complementary sequences. sRNAs from both plant and animal hosts have been recognized as regulators in host-microbial interaction (*5*–*8*). Although sRNAs are also present in various fungi and oomycetes, including many pathogens (*9*–*14*), it has not been clear whether they regulate host-pathogen interaction.

To explore the role of *B. cinerea* sRNAs in pathogenicity, we profiled sRNA libraries prepared from *B. cinerea* (strain B05.10)–infected *Arabidopsis thaliana* Col-0 leaves collected at 0, 24, 48, and 72 hours after inoculation and from *B. cinerea*–infected *Solanum lycopersicum* (tomato) leaves and fruits at 0, 24, and 72 hours after inoculation. sRNA libraries prepared from *B. cinerea* mycelia, conidiospores, and total biomass after 10 days of culture were used as controls. By using 100 normalized reads per million *B. cinerea* sRNA reads as a cutoff, we identified a total of 832 sRNAs that were present in both *B. cinerea*–infected *Arabidopsis* and *S. lycopersicum* libraries and had more reads in these libraries than in the cultured *B. cinerea* libraries, with sequences exactly matching the *B. cinerea* B05.10 genome (*15*) but not *Arabidopsis* or *S. lycopersicum* genomes or cDNA (tables S1 to S3). The closest sequence matches in *Arabidopsis* or *S. lycopersicum* contained a minimum of two mismatches. Among them, 27 had predicted microRNA (miRNA)–like precursor structures. A similar number of miRNA-like sRNAs were found in *Sclerotinia sclerotiorum* (*9*). We found that 73 Bc-sRNAs could target host genes in both *Arabidopsis* and *S. lycopersicum* under stringent target prediction criteria (tables S3). Among them, 52 were derived from six retrotransposon long terminal repeats (LTR) loci in the *B. cinerea* genome, 13 were from intergenic regions of 10 loci, and eight were mapped to five protein-coding genes.

Some of the predicted plant targets, such as mitogen-activated protein kinases (MAPKs), are likely to function in plant immunity. To test whether Bc-sRNAs could indeed suppress host genes during infection, three Bc-sRNAs (Bc-siR3.1, Bc-siR3.2, and Bc-siR5) were selected for further characterization (table S2). These Bc-sRNAs were among the most abundant sRNAs that were 21 nucleotides (nt) in length and had potential targets likely to be involved in plant immunity in both *Arabidopsis* and *S. lycopersicum*. These sRNAs were also enriched after infection (Fig. 1, A and B; fig. S1; and table S2) and were the major sRNA products from their encoding loci, LTR retrotransposons (fig. S1). Bc-siR3.1 and Bc-siR3.2 were derived from the same locus with a 4-nt shift in sequence.

To determine whether Bc-sRNAs could trigger silencing of host genes, we examined the transcript levels of the predicted target genes after *B. cinerea* infection. The following *Arabidopsis* genes were targeted in the coding regions and were suppressed after *B. cinerea* infection: *mitogen activated protein kinase 2* (*MPK2*) and *MPK1*, which are targeted

[1]Department of Plant Pathology and Microbiology, University of California, Riverside, CA 92521, USA. [2]Center for Plant Cell Biology, University of California, Riverside, CA 92521, USA. [3]Institute for Integrative Genome Biology, University of California, Riverside, CA 92521, USA. [4]Department of Biological Science and Technology, National Chiao Tung University, Hsin-Chu 300, Taiwan. [5]College of Horticulture, Shenyang Agricultural University, Shenyang, Liaoning 110866, China. [6]Department of Nematology, University of California, Riverside, CA 92521, USA. [7]Institute of Bioinformatics and Systems Biology, National Chiao Tung University, Hsin-Chu 300, Taiwan.

*These authors contributed equally to this work.
†Present address: College of plant protection, Nanjing Agricultural University, Nanjing, Jiangsu 210095, China.
‡Corresponding author. E-mail: hailingj@ucr.edu

by Bc-siR3.2; an oxidative stress-related gene, *peroxiredoxin* (*PRXIIF*), which is targeted by Bc-siR3.1; and *cell wall-associated kinase* (*WAK*), which is targeted by Bc-siR5 (Fig. 1C). In contrast, the plant defense marker genes *PDF1.2* and *BIK1* (*16*), which do not contain the Bc-sRNA target sites, were highly induced upon *B. cinerea* infection (Fig. 1C). We conclude that suppression of some but not all genes is a result of sequence-specific sRNA interaction and not due to cell death within infected lesions. Bc-siR3.2, which silences *Arabidopsis MPK1* and *MPK2*, was enriched also in *S. lycopersicum* leaves upon *B. cinerea* infection (Fig. 1B) and was predicted to target another member of the MAPK signaling cascade in *S. lycopersicum*, *MAPKKK4* (table S2). Expression of *MAPKKK4* was indeed suppressed upon *B. cinerea* infection (Fig. 1D).

To confirm that the suppression of the targets was indeed triggered by Bc-sRNAs, we performed coexpression assays in *Nicotiana benthamiana*. Expression of hemagglutinin (HA)–epitope tagged MPK2, MPK1, and WAK was reduced when they were coexpressed with the corresponding Bc-sRNAs but not when coexpressed with *Arabidopsis* miR395, which shared no sequence similarity (Fig. 1E). The silencing was abolished, however, when the target genes carried a synonymously mutated version of the relevant Bc-sRNA target sites (Fig. 1E and fig. S2A). We also observed suppression of yellow fluorescent protein (YFP)–tagged target MPK2 by *B. cinerea* infection at 24 hours after inoculation (Fig. 1F and fig. S2B); when the Bc-siR3.2 target site of *MPK2* was mutated, infection by *B. cinerea* failed to suppress its expression (Fig. 1F and fig. S2B). Thus, Bc-siR3.2 delivered from *B. cinerea* is sufficient for inducing silencing of wild-type *MPK2* but cannot silence target site–mutated *MPK2*. Similarly, of the YFP-sensors with wild-type or mutated Bc-siR3.2 target sites (fig. S2C), only the wild-type sensor was suppressed after *B. cinerea* infection (Fig. 1G).

To test the effect of Bc-sRNAs on host plant immunity, we generated transgenic *Arabidopsis* plants that ectopically expressed Bc-siR3.1, Bc-siR3.2, or Bc-siR5 using a plant artificial miRNA vector (Fig. 2A) (*17*). These Bc-sRNA expression (Bc-sRNAox) lines showed normal morphology and development without pathogen challenge when compared with the wild-type plants, and expression of the target genes was suppressed (Fig. 2B). With pathogen challenge, all of the Bc-sRNAox lines displayed enhanced susceptibility to *B. cinerea* (Fig. 2, C and E). The results indicate that these Bc-sRNAs play a positive role in *B. cinerea* pathogenicity.

Enhanced disease susceptibility of the Bc-sRNAox lines suggests that the target genes of these Bc-sRNAs are likely to be involved in host immunity against *B. cinerea*. Plants with mutated target genes showed normal morphology and development without pathogen challenge. The *Arabidopsis* targets of Bc-siR3.2, *MPK1* and *MPK2*, are homologs that share 87% amino acid identity. These genes are functionally redundant and are coactivated in response to various stress factors (*18*). The *mpk1 mpk2* double mutant exhibited enhanced susceptibility to *B. cinerea* (Fig. 2, D and E). A transferred-DNA knockout mutant of the Bc-siR5 target *WAK* (SALK_089827) (fig. S3A) also displayed enhanced susceptibility to *B. cinerea* (Fig. 2, D and E). Consistent

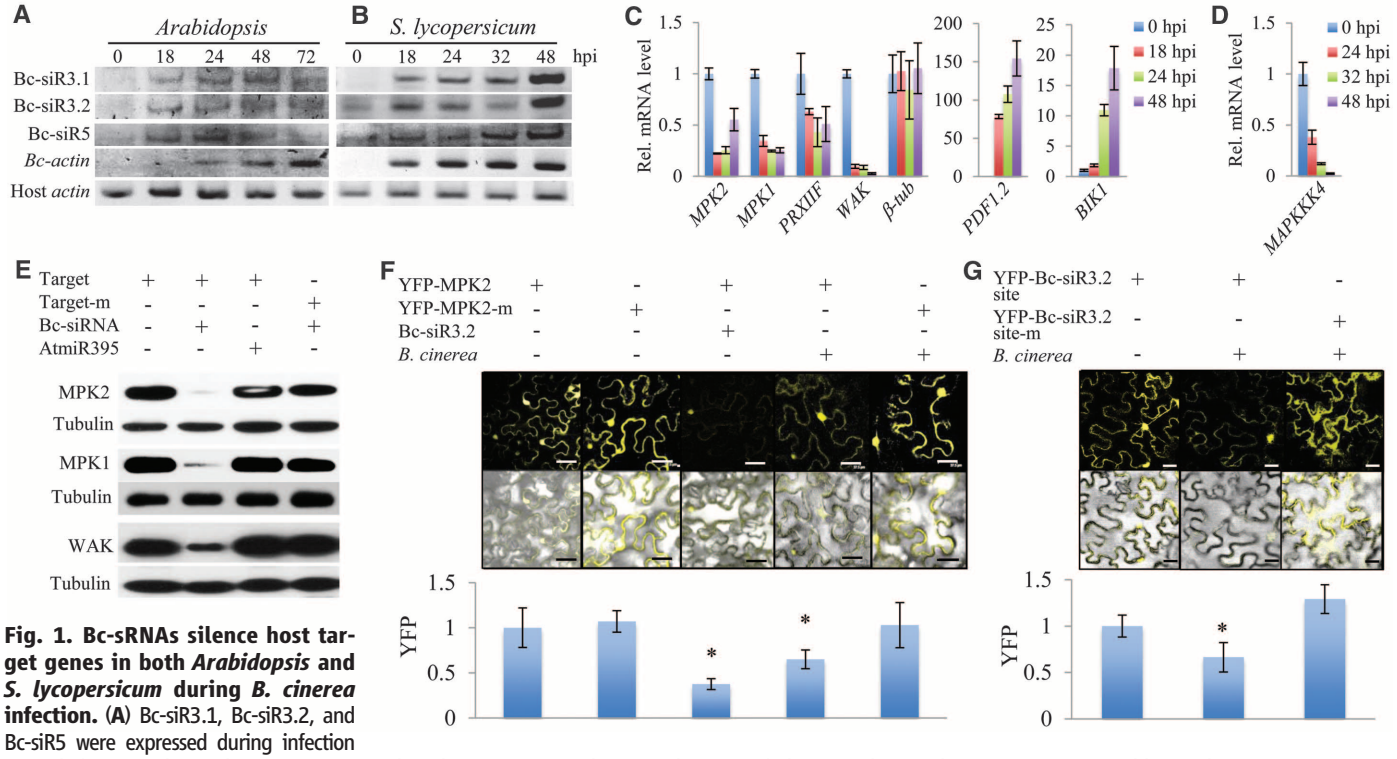

Fig. 1. Bc-sRNAs silence host target genes in both *Arabidopsis* and *S. lycopersicum* during *B. cinerea* infection. (**A**) Bc-siR3.1, Bc-siR3.2, and Bc-siR5 were expressed during infection of *Arabidopsis* as detected at 18, 24, 48, and 72 hours after inoculation and (**B**) *S. lycopersicum* leaves at 18, 24, 32, 48 hours after inoculation by means of reverse transcription polymerase chain reaction (RT-PCR). Actin genes of *B. cinerea*, *Arabidopsis*, and *S. lycopersicum* were used as internal controls. Similar results were obtained from three biological replicates. (**C**) The *Arabidopsis* targets of Bc-sRNAs were suppressed after *B. cinerea* infection. *PDF1.2*, *BIK1*, and β-*tubulin* were used as controls. (**D**) The *S. lycopersicum* target gene *MAPKKK4* was suppressed upon *B. cinerea* infection. Expression [(C) and (D)] was measured by means of quantitative RT-PCR by using actin as an internal control. Error bars indicate SD of three technical replicates. Similar results were seen in three biological replicates. (**E**) Coexpression of Bc-siR3.2 or Bc-siR5 with their host targets (HA-tagged) in *N. benthamiana* revealed target silencing by means of Western blot analysis. Coexpression of AtmiR395 or target site–mutated versions of target genes was used as controls. (**F**) Expression of *YFP-MPK2* or its synonymously mutated version (*YFP-MPK2-m*) after infection of *B. cinerea* was observed with confocal microscopy. Coexpression of *YFP-MPK2* and Bc-siR3.2 was used as a control. (**G**) Expression of the *YFP* sensors carrying a Bc-siR3.2 target site of *MPK2* or a Bc-siR3.2 target site-m was analyzed after infection of *B. cinerea*. Samples were examined at 24 hours after inoculation. (Top) YFP. (Bottom) YFP/bright field overlay. Scale bars [(F) and (G)], 37.5 μm. Error bars indicate SD of 20 images [(F) and (G)]. The asterisk indicates significant difference (two-tail *t*-test; $P < 0.01$). Similar results were obtained in three biological replicates in (E) to (G).

with this, Bc-sRNAox lines as well as *mpk1 mpk2* and *wak* showed lower induction of the defense marker gene *BIK1* (fig. S3B). These results suggest that the *MPK1*, *MPK2*, and *WAK* genes, all of which are targeted by Bc-sRNAs, participate in the plant's immune response to *B. cinerea*. To determine whether *MAPKKK4* is involved in *S. lycopersicum* defense response against *B. cinerea*, we applied the virus-induced gene silencing (VIGS) approach to knock down *MAPKKK4* in *S. lycopersicum* using tobacco rattle virus (TRV) (fig. S4A) (*19*). VIGS of TRV-*MAPKKK4* caused a dwarf phenotype (fig. S4B). The *MAPKKK4*-silenced plants showed enhanced disease susceptibility in response to *B. cinerea* and contained >15 times more fungal biomass than that of the control plants (Fig. 2F). We conclude that Bc-sRNAs silence plant genes to suppress host immunity during early infection.

These fungal sRNAs hijack the plant's own gene silencing mechanism. Sixty-three of the 73 Bc-sRNAs that had predicted *Arabidopsis* and *S. lycopersicum* targets were 20 to 22 nt in length with a 5′ terminal U (table S3). This sRNA structure is favored for binding to AGO1 in *Arabidopsis* (*20*, *21*). In order to determine whether Bc-sRNAs act through *Arabidopsis* AGO1, we immunoprecipitated AGO1 from *B. cinerea*–infected *Arabidopsis* collected at 24, 32, and 48 hours after inoculation and analyzed the AGO1-associated sRNAs. Bc-siR3.1, Bc-siR3.2, and Bc-siR5 were clearly detected in the AGO1-associated fraction pulled down from the infected plant samples but hardly in the control (Fig. 3A) or in the AGO2- and AGO4-associated sRNA fractions (fig. S5). The sRNAs that had no predicted plant targets or had predicted targets that were not down-regulated by *B. cinerea* infection were not found in the AGO1-associated fractions (fig. S6).

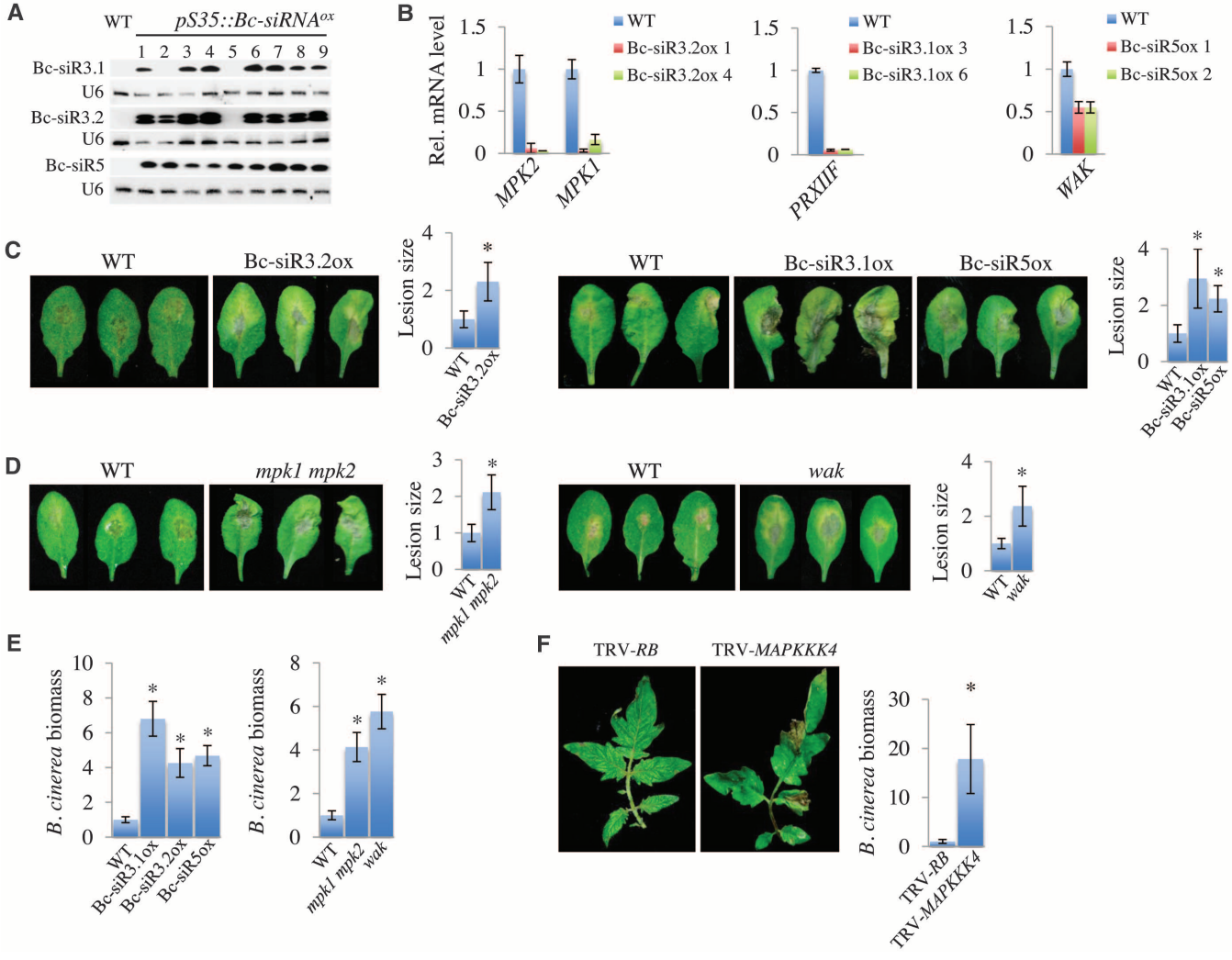

Fig. 2. Bc-sRNAs trigger silencing of host targets that are involved in host immunity. (**A**) Expression of Bc-siR3.1, BcsiR3.2, or Bc-siR5 in transgenic *Arabidopsis* ectopically expressing Bc-sRNAs under the Cauliflower Mosaic Virus promoter 35S (Bc-sRNAox) was examined by means of Northern blot analysis. Highly expressed lines were selected for the following experiments. (**B**) Bc-sRNAox lines showed constitutive silencing of respective Bc-sRNA target genes measured with quantitative RT-PCR. Two independent lines for each Bc-sRNA were examined. Similar results were observed in two generations of the selected transgenic lines. (**C**) Bc-sRNAox plants exhibited enhanced disease susceptibility to *B. cinerea* as compared with wild type. (**D**) Loss-of-function mutants of Bc-siR3.2 and Bc-siR5 targets *mpk1 mpk2* and *wak* displayed enhanced disease susceptibility. In all pathogen assays [(C) and (D)], lesion sizes were measured at 96 hours after inoculation. Error bars indicate the SD of 20 leaves. (**E**) Biomass of *B. cinerea* was measured with quantitative PCR at 96 hours after inoculation. Error bars indicate SD of three technical replicates. For (C), (D), and (E), similar results were obtained from three biological repeats. (**F**) VIGS of *MAPKKK4* exhibited enhanced disease susceptibility to *B. cinerea* in *S. lycopersicum* (examined at 72 hours after inoculation) as compared with control plants (TRV-*RB*). *RB* is a late-blight resistance gene that is not present in tomato. We chose to use a TRV vector with a fragment from a foreign gene as a control to eliminate the potential side effect of viral disease symptoms caused by TRV empty vector. Spray inoculation was used because silencing sectors are not uniform within the VIGS plants. Three sets of experiments with each of 6 to 10 plants for each construct were performed, and similar results were obtained. The asterisk indicates significant difference (two-tail *t*-test, $P < 0.01$) in (C) to (F).

If AGO1 plays an essential role in Bc-sRNA–mediated host gene silencing, we would expect to see reduced disease susceptibility in the *ago1* mutant because these Bc-sRNAs could no longer suppress host immunity genes. For plants carrying the *ago1-27* mutant allele (*22*) and were inoculated with *B. cinerea*, the disease level was significantly less than on the wild type (Fig. 3B and fig. S7A). Consistent with this, *BIK1* induction was increased compared with that of the wild-type (fig. S7B). Furthermore, the expression of Bc-siR3.2 targets *MPK2* and *MPK1*, Bc-siR3.1 target *PRXIIF*, and Bc-siR5 target *WAK* in *ago1-27* was not suppressed compared with those in wild-type infected plants after *B. cinerea* infection (Fig. 3C). On the contrary, *Arabidopsis* miRNA biogenesis mutant *dicer-like* (*dcl*) *1-7* that shows similar morphological defects to *ago1-27* exhibited an enhanced disease level to *B. cinerea* (Fig. 3D). These results suggest that the increased resistance phenotype we observed in *ago1-27* is not caused by any reduced vigour or pleiotropic phenotype but was due to the function of the Bc-sRNAs, and that *Arabidopsis* DCL1 is not required for the function of Bc-sRNAs. Thus, Bc-sRNAs evidently hijacked host RNAi machinery by loading into AGO1; the complex in turn suppressed host immunity genes.

To delete the siR3 and siR5 loci from the *B. cinerea* genome by homologous recombination would be an ideal way to confirm their function; however, it is not feasible because siR3 is from a LTR with three copies and siR5 is from a LTR with 13 copies. To better understand the function and biogenesis of the Bc-sRNAs, we chose to knock out the *B. cinerea* DCL genes, which encode the core sRNA processing enzymes. *B. cinerea* strain B05.10 possesses two Dicer-like genes (*Bc-DCL1* and *Bc-DCL2*) (fig. S8). We generated *dcl1* and *dcl2* single and *dcl1 dcl2* double knockout mutant strains through homologous recombination (fig. S9, A and B). We found that *dcl1* and *dcl2* single mutants showed reduced growth and delayed sporulation (fig. S9C). The *dcl1 dcl2* double mutant displayed a more obvious phenotype than that of each of the single mutants, suggesting partial functional redundancy between DCL1 and DCL2 in *B. cinerea*. Bc-siR3.1, Bc-siR3.2, and Bc-siR5 could not be detected in the *dcl1 dcl2* double mutant (Fig. 4A), indicating that they were DCL-dependent, whereas two other Bc-sRNAs, Bc-milR2 and Bc-siR1498, could still be detected in *dcl1 dcl2* double mutant (fig. S9D). Fungi have diverse sRNA biogenesis pathways, and not all sRNAs are DCL-dependent (*12*). The *dcl1 dcl2* double mutant caused significantly smaller lesions than those of the wild type or *dcl1* and *dcl2* single mutants on both *Arabidopsis* and *S. lycopersicum* leaves (Fig. 4, B and C), in consistence with the significantly reduced fungal biomass at 72 hours after inoculation in *Arabidopsis* and 48 hours after inoculation in *S. lycopersicum* (fig. S10), which indicates that the virulence of the *dcl1 dcl2* mutant was greatly reduced. These results further support the conclusion that Bc-sRNAs—particularly Bc-siR3.1, Bc-siR3.2, and Bc-siR5, which depend on *B. cinerea* DCL function—contribute to the pathogenicity of *B. cinerea*. Mutation of *dcl1* or *dcl2* in *B. cinerea* caused delayed growth and sporulation (fig. S9C) but had no effect on pathogenicity (Fig. 4, B and C). Furthermore, expression of the YFP sensor carrying the Bc-siR3.2 target site in *N. benthamiana* was silenced when infected

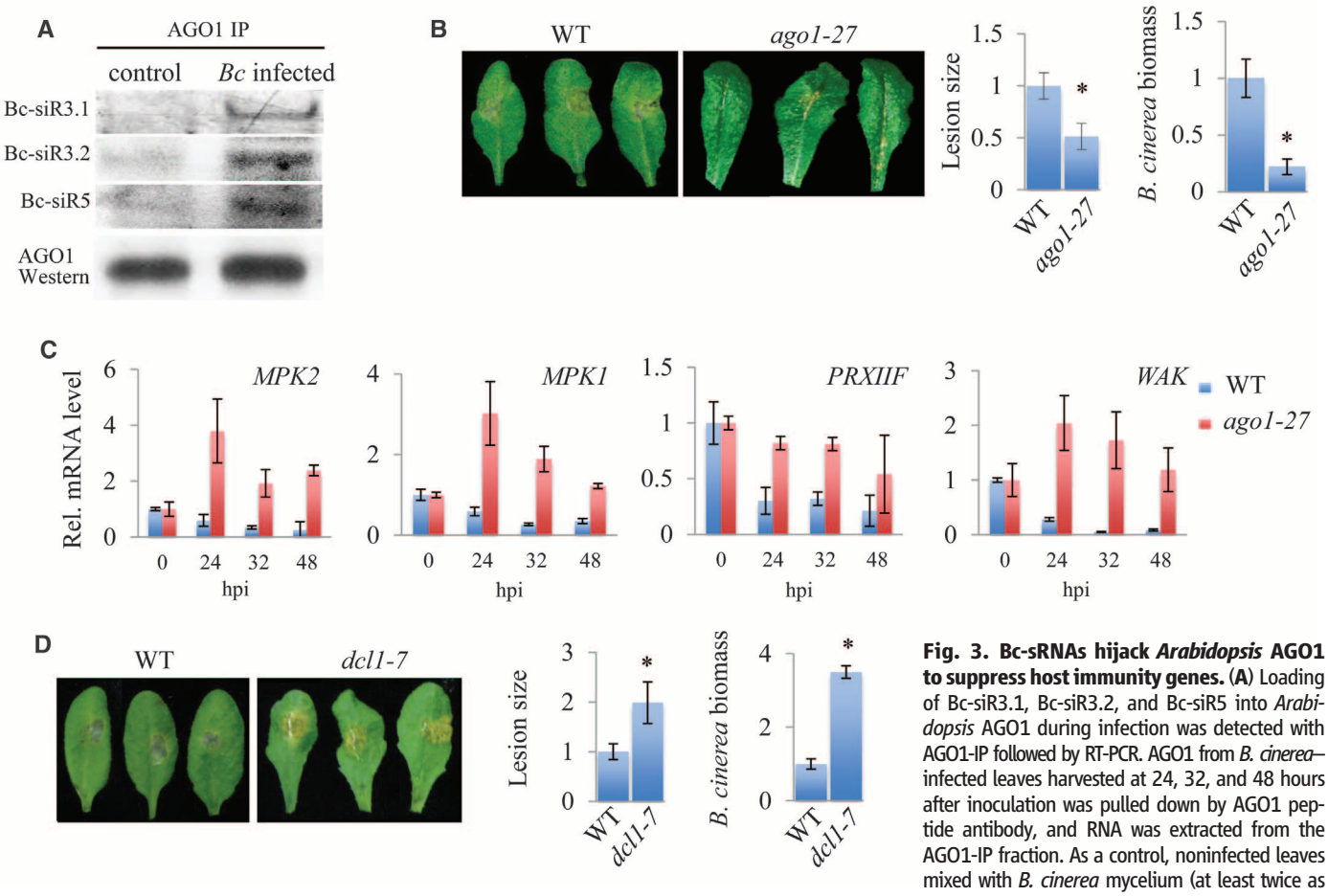

Fig. 3. Bc-sRNAs hijack *Arabidopsis* AGO1 to suppress host immunity genes. (**A**) Loading of Bc-siR3.1, Bc-siR3.2, and Bc-siR5 into *Arabidopsis* AGO1 during infection was detected with AGO1-IP followed by RT-PCR. AGO1 from *B. cinerea*–infected leaves harvested at 24, 32, and 48 hours after inoculation was pulled down by AGO1 peptide antibody, and RNA was extracted from the AGO1-IP fraction. As a control, noninfected leaves mixed with *B. cinerea* mycelium (at least twice as much as that in *B. cinerea*–infected leaves at 48 hours after inoculation) were used to rule out any binding between AGO1 and Bc-sRNAs during the experimental procedures. Similar results were obtained from at least three biological repeats. (**B**) *Arabidopsis ago1-27* exhibited reduced disease susceptibility to *B. cinerea* as compared with the wild type. Lesion size of at least 20 leaves and fungal biomass were measured at 96 hours after inoculation. (**C**) Silencing of *MPK2*, *MPK1*, *PRXIIF*, and *WAK* during *B. cinerea* infection was abolished in *ago1-27*. (**D**) *Arabidopsis dcl1-7* exhibited enhanced disease susceptibility to *B. cinerea* as compared with the wild type. Similar results were obtained from three biological repeats [(B) to (D)]. The asterisk indicates significant difference (two-tail *t*-test, $P < 0.01$) in (B) and (D).

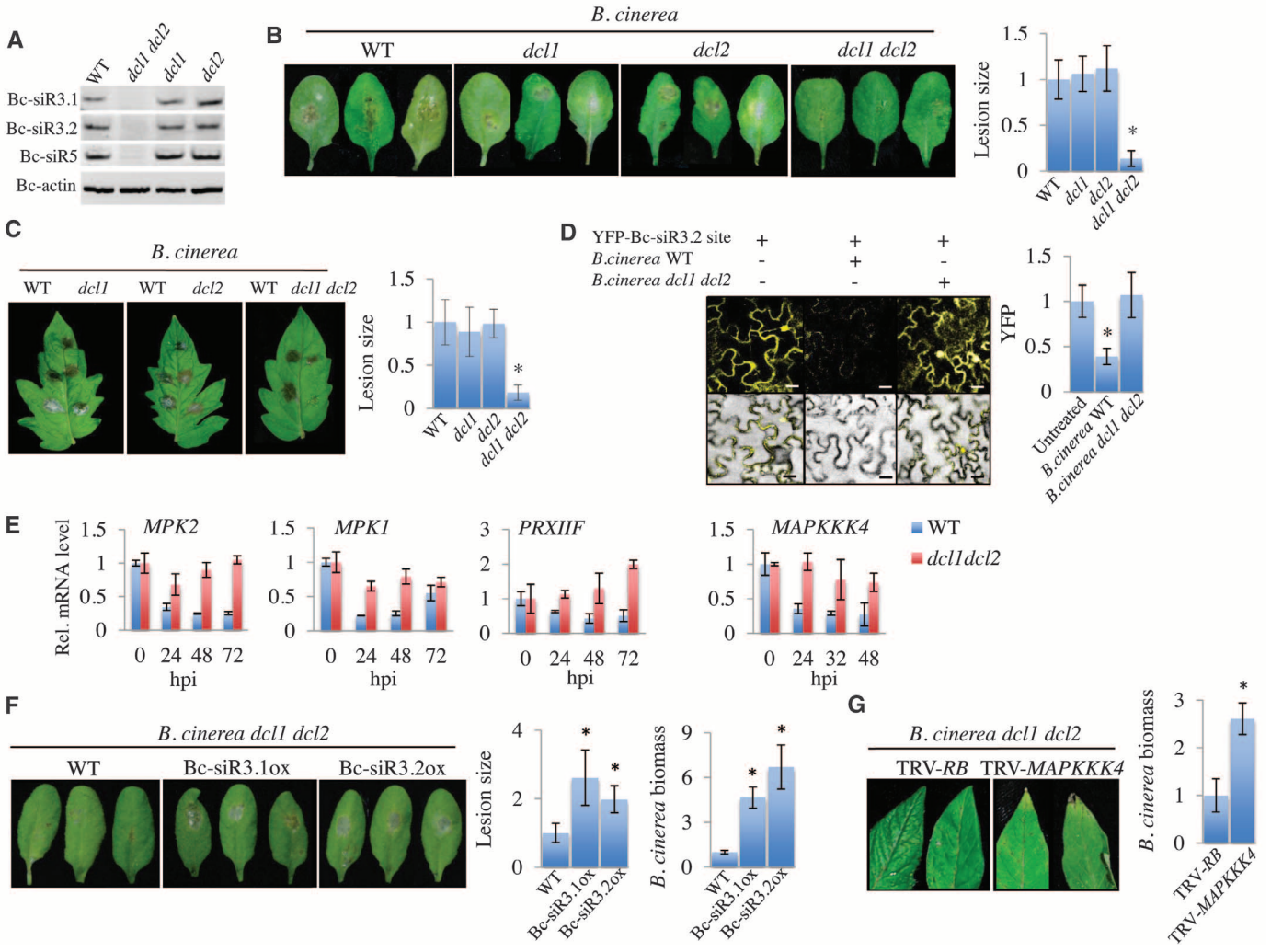

Fig. 4. *B. cinerea dcl1 dcl2* double mutant is compromised in virulence. (**A**) *B. cinerea dcl1 dcl2* double mutant, but not *dcl1* or *dcl2* single mutants, was impaired in generating Bc-siR3.1, Bc-siR3.2, and Bc-siR5 as revealed with RT-PCR. *B. cinerea dcl1 dcl2* double mutant, but not *dcl1* or *dcl2* single mutants, produced much weaker disease symptoms than did the wild type in (**B**) *Arabidopsis* and (**C**) *S. lycopersicum*, as demonstrated by the lesion size measured of 20 leaves at 96 and 48 hours after inoculation, respectively. Similar results were obtained from three biological repeats. (**D**) Expression of the sensor *YFP*-Bc-siR3.2 target site was silenced by wild-type *B. cinerea* upon infection, but not by the *dcl1 dcl2* mutant at 24 hours after inoculation. Scale bar, 75 μm. Error bars indicate SD of 20 images. Experiments were repeated two times with similar results. (**E**) *B. cinerea dcl1 dcl2* mutant was compromised in suppression of *MPK2*, *MPK1*, and *PRXIIF* in *Arabidopsis* and *MAPKKK4* in *S. lycopersicum*. Similar results were seen in two biological repeats. (**F**) *Arabidopsis* Bc-siR3.1ox and Bc-siR3.2ox lines were more susceptible to *B. cinerea dcl1 dcl2* strain than was Col-0 wild type. (**G**) Enhanced disease phenotype of *dcl1 dcl2* infection was also observed on TRV-*MAPKKK4*–silenced *S. lycopersicum* plants. Experiments in (F) and (G) were repeated three times with similar results. *B. cinerea* biomass was quantified at 96 hours after inoculation. The asterisk [in (B), (C), (D), (F), and (G)] indicates significant difference (two-tail *t*-test; $P < 0.01$).

with wild-type *B. cinerea*. The suppression was abolished when inoculated with the *dcl1 dcl2* strain (Fig. 4D), indicating that the *dcl1 dcl2* double mutant was unable to generate Bc-siR3.2 to suppress the target. We also confirmed the inability of *dcl1 dcl2* to suppress Bc-siR3.1 and Bc-siR3.2 target genes *MPK2*, *MPK1*, and *PRXIIF* in *Arabidopsis* and *MAPKKK4* in tomato upon infection (Fig. 4E). Consistent with this, the *dcl1 dcl2* virulence was partially restored when infected on *Arabidopsis* Bc-siR3.1ox and Bc-siR3.2ox plants as well as in tomato TRV-*MAPKKK4*–silenced plants (Fig. 4, F and G).

Animal and plant pathogens have evolved virulence or effector proteins to counteract host immune responses. Various protein effectors have been predicted or discovered in fungal or oomycete pathogens from whole-genome sequencing and secretome analysis (*2*, *3*), although delivery mechanisms are still under active investigation (*23*–*27*). Here, we show that sRNAs as well can act as effectors through a mechanism that silences host genes in order to debilitate plant immunity and achieve infection. The sRNAs from *B. cinerea* hijack the plant RNAi machinery by binding to AGO proteins, which in turn direct host gene silencing. Another fungal plant pathogen, *Verticllium dahliae*, also depends on AGO1 function for its pathogenicity (*28*). The implications of these findings may extend beyond plant gray mold disease caused by *B. cinerea* and suggest an extra mechanism underlying pathogenesis promoted by sophisticated pathogens with the capability to generate and deliver small regulatory RNAs into hosts to suppress host immunity.

References and Notes

1. H. Ashida *et al.*, *Curr. Opin. Microbiol.* **14**, 16–23 (2011).
2. M. Rafiqi, J. G. Ellis, V. A. Ludowici, A. R. Hardham, P. N. Dodds, *Curr. Opin. Plant Biol.* **15**, 477–482 (2012).
3. T. O. Bozkurt, S. Schornack, M. J. Banfield, S. Kamoun, *Curr. Opin. Plant Biol.* **15**, 483–492 (2012).
4. H. Hilbi, A. Haas, *Traffic* **13**, 1187–1197 (2012).
5. S. Katiyar-Agarwal, H. Jin, *Annu. Rev. Phytopathol.* **48**, 225–246 (2010).
6. V. Ruiz-Ferrer, O. Voinnet, *Annu. Rev. Plant Biol.* **60**, 485–510 (2009).
7. B. Wessner, L. Gryadunov-Masutti, H. Tschan, N. Bachl, E. Roth, *Exerc. Immunol. Rev.* **16**, 22–39 (2010).

8. X. Zhang *et al.*, *Mol. Cell* **42**, 356–366 (2011).
9. J. Zhou *et al.*, *Mol. Gen. Genet.* **287**, 275–282 (2012).
10. D. Qutob, B. Patrick Chapman, M. Gijzen, *Nature Comm.* **4**, 1349 (2013).
11. N. Jiang, Y. Yang, G. Janbon, J. Pan, X. Zhu, *PLoS ONE* **7**, e52734 (2012).
12. H. C. Lee *et al.*, *Mol. Cell* **38**, 803–814 (2010).
13. C. C. Nunes *et al.*, *BMC Genomics* **12**, 288 (2011).
14. V. Raman *et al.*, *BMC Genomics* **14**, 326 (2013).
15. J. Amselem *et al.*, *PLOS Genet.* **7**, e1002230 (2011).
16. P. Veronese *et al.*, *Plant Cell* **18**, 257–273 (2006).
17. R. Schwab, S. Ossowski, M. Riester, N. Warthmann, D. Weigel, *Plant Cell* **18**, 1121–1133 (2006).
18. D. Ortiz-Masia, M. A. Perez-Amador, J. Carbonell, M. J. Marcote, *FEBS Lett.* **581**, 1834–1840 (2007).
19. Y. L. Liu, M. Schiff, S. P. Dinesh-Kumar, *Plant J.* **31**, 777–786 (2002).
20. S. J. Mi *et al.*, *Cell* **133**, 116–127 (2008).
21. T. A. Montgomery *et al.*, *Cell* **133**, 128–141 (2008).
22. J. B. Morel *et al.*, *Plant Cell* **14**, 629–639 (2002).
23. S. D. Kale *et al.*, *Cell* **142**, 284–295 (2010).
24. S. Wawra *et al.*, *Curr. Opin. Microbiol.* **15**, 685–691 (2012).
25. M. Rafiqi *et al.*, *Plant Cell* **22**, 2017–2032 (2010).
26. S. Schornack *et al.*, *Proc. Natl. Acad. Sci. U.S.A.* **107**, 17421–17426 (2010).
27. S. Wawra *et al.*, *Proc. Natl. Acad. Sci. U.S.A.* **109**, 2096–2101 (2012).
28. U. Ellendorff, E. F. Fradin, R. de Jonge, B. P. Thomma, *J. Exp. Bot.* **60**, 591–602 (2009).

Acknowledgments: We thank Y. Qi for AGO1 antibody; J. Carrington for the AGO1 and AGO2 tagged lines; H. Vaucheret for *ago1-27* mutant; M. J. Marcote for *mpk1 mpk2* seeds; and P. Karlovsky for pPK2 binary vector and *A. tumefaciens* strain AGL1 for *B. cinerea* transformation and gene knockout. This work was supported by an NIH grant (R01 GM093008), an NSF Career Award (MCB-0642843), an NSF award (IOS-1257576), and an AES-CE award (PPA-7517H) to H.J.; National Science Council of the Republic of China (NSC 101-2311-B-009-003-MY3 and NSC 100-2627-B-009-002) and UST-UCSD I-RiCE Program (NSC 101-2911-I-009-101) grants to H.-D.H.

Supplementary Materials

www.sciencemag.org/content/342/6154/118/suppl/DC1
Materials and Methods
Fig. S1 to S10
Tables S1 to S4
References (*29*–*32*)

26 April 2013; accepted 19 August 2013
10.1126/science.1239705

Crystal Structure of Na^+, K^+-ATPase in the Na^+-Bound State

Maria Nyblom,[1,2]*† Hanne Poulsen,[1,2,3]*‡ Pontus Gourdon,[1,2,3]* Linda Reinhard,[1,2]§ Magnus Andersson,[4] Erik Lindahl,[4,5] Natalya Fedosova,[1,6] Poul Nissen[1,2,3]‡

The Na^+, K^+–adenosine triphosphatase (ATPase) maintains the electrochemical gradients of Na^+ and K^+ across the plasma membrane—a prerequisite for electrical excitability and secondary transport. Hitherto, structural information has been limited to K^+-bound or ouabain-blocked forms. We present the crystal structure of a Na^+-bound Na^+, K^+-ATPase as determined at 4.3 Å resolution. Compared with the K^+-bound form, large conformational changes are observed in the α subunit whereas the β and γ subunit structures are maintained. The locations of the three Na^+ sites are indicated with the unique site III at the recently suggested IIIb, as further supported by electrophysiological studies on leak currents. Extracellular release of the third Na^+ from IIIb through IIIa, followed by exchange of Na^+ for K^+ at sites I and II, is suggested.

The Na^+, K^+–adenosine triphosphatase (ATPase) is typically a ternary complex of a large catalytic α subunit associated with two smaller subunits, β and γ (Fig. 1A). Different isoforms combine to form kinetically distinct complexes in different cells and tissues (*1*). During the ATP-driven transport cycle, three cytoplasmic Na^+ are exported in exchange for two extracellular K^+ through alternating E1/E1P and E2P/E2 states (Fig. 1B), where E1 and E2 denote high affinity for sodium and potassium ions, respectively, and P is phosphorylated. Intracellular Na^+ and ATP binding stimulate phosphorylation of a conserved aspartic acid residue (Asp^{369} in pig α_1 isoform; see alignment in fig. S1), forming the sodium-occluded $[Na_3]$E1P–adenosine diphosphate (ADP) state. Conformational changes and ADP release open an extracellular pathway in the E2P state, and Na^+ release and K^+ binding stimulate dephosphorylation, yielding the potassium-occluded $[K_2]$E2.P_i and $[K_2]$E2 states. Subsequent ATP binding and cytoplasmic K^+ release lead to the sodium-bound E1 states.

Previously, K^+-bound crystal structures representing the occluded E2.P_i state as mimicked by magnesium fluoride ($[K_2]$E2-MgF_x) (*2*, *3*) and structures with the inhibitory steroid ouabain (low-affinity $[K_2]$E2-MgF_x and high-affinity [Mg]E2P) have been elucidated (*4*, *5*). The intracellular C-terminal tail of the α subunit plays an important role in Na^+ binding (*2*, *6*–*10*), apparently by controlling an ion pathway (*6*, *7*), through a mechanism affected by many of the α_2 and α_3 isoform mutations that are associated with neurological diseases (*11*, *12*). However, further elucidation of the transport mechanism of the Na^+, K^+-ATPase has been limited by the lack of a structure of the Na^+-bound state, and in particular the location of the third Na^+ site has remained unsettled.

We present here the crystal structure determined at 4.3 Å resolution of the Na^+, K^+-ATPase in the $[Na_3]$E1P-ADP state (pig renal $\alpha_1\beta_1\gamma$ enzyme) as mimicked by an ADP-AlF_4^- complex (materials and methods and table S1) for which Na^+ saturation was further stabilized by the presence of oligomycin. The structure was determined from an unbiased electron density map derived by single isomorphous replacement with anomalous scattering (SIRAS), using hexatantalum dodecabromide (Ta_6Br_{12}) derivatized crystals, followed by density modification procedures (Fig. 1C and fig. S2). Model building using sharpened maps and restrained refinement produced a final model with R_{work} and R_{free} of 26.1 and 28.8%, respectively. The structure represents two nearly identical complexes in the asymmetric unit (chains A-B-G and C-D-E) and displays bilayer features in the electron density (figs. S2 to S4).

The ability of the E1-AlF_4^--ADP complex to occlude three Na^+ under crystallization-like conditions was confirmed by time-course measurements of $^{22}Na^+$ deocclusion at 0°C (Fig. 1F). The monoexponential fit resulted in the maximal number of 2.5 nmol of Na^+ per nmol of ADP binding sites (i.e., 83% occupancy) at 1 mM $^{22}Na^+$ and the deocclusion rate constant of 0.02 s^{-1}. Assuming a Hill coefficient of 3 for the cooperative Na^+ binding, the ion concentration required for the half-maximal saturation of the sites ($K_{0.5}$ for Na^+) was calculated to be 0.58 mM, consistent with previous findings (*13*). Thus, Na^+ concentration under crystallization conditions (>80 mM) was more than two orders of magnitude higher than the $K_{0.5}$, enough to saturate all three sites.

The α subunit represents a Na^+-occluded form of the transmembrane (TM) domain, with the cytoplasmic A, P, and N domains arranged for phosphorylation (Fig. 1, C and D) as observed for sarcoplasmic reticulum Ca^{2+} ATPase 1a (SERCA1a) in the equivalent, Ca^{2+}-occluded state (fig. S4B) (*14*–*16*). Thus, compared with K^+-bound forms, the α subunit is characterized by a different organization of the TM helices and a compact configuration of the cytoplasmic domains activating the phosphorylation site (Fig. 1, C and D, and fig. S5). Relative to the P domain, the A domain has undergone a rigid-body rota-

[1]Centre for Membrane Pumps in Cells and Disease–PUMPkin, Danish National Research Foundation, DK-8000 Aarhus, Denmark. [2]Department of Molecular Biology and Genetics, Aarhus University, Gustav Wieds Vej 10c, DK-8000 Aarhus, Denmark. [3]Danish Research Institute for Translational Neuroscience–DANDRITE, Nordic-EMBL Partnership of Molecular Medicine, Aarhus, Denmark. [4]Science for Life Laboratory, Theoretical and Computational Biophysics, Department of Theoretical Physics, Swedish e-Science Research Center, KTH Royal Institute of Technology, SE-171 21 Solna, Sweden. [5]Science for Life Laboratory, Department of Biochemistry and Biophysics, Stockholm University, SE-106 91 Stockholm, Sweden. [6]Department of Biomedicine, Aarhus University, Ole Worms Allé 4, Building 1182, DK-8000 Aarhus, Denmark.

*These authors contributed equally to this work.
†Present address: Novo Nordisk A/S, Novo Nordisk Park, B9.2.31, DK-2760 Maalov, Denmark.
‡Corresponding author. E-mail: hp@mb.au.dk (H.P.); pn@mb.au.dk (P.N.)
§Present address: Department of Cell and Molecular Biology, Karolinska Institutet, Box 285, SE-171 77 Stockholm, Sweden.